Simulation and Design of an Oven for PET Blow Molding Machines

Carlo A. Seneci[1], Maurizio Mor[1*], Davide Fausti[1], Gianluigi Petrogalli[1], Carlo Remino[1] and Vanni Zacché[2]
[1]Polibrixia S.r.l – via Branze, 45 Brescia, Italy *maurizio.mor@polibrixia.it
[2]SMI Group S.p.a. – via Piazzalunga, 30 San Giovanni Bianco - BG, Italy

Abstract: This paper presents the study and design of a new generation oven for PET blow-molding machines. The design faced several technical challenges such as: the temperature distribution in the critical areas, the sharp curvature radius, the high PET thermal inertia and the presence of boundary elements, which affected the overall performances. In fact the study started with a state of the art evaluation that was useful to align the COMSOL model with the industrial practice giving the possibility to improve the design. The work included an analysis of the preform material and geometry influence on the heating and transformation process, followed by the definition of the model to implement in the simulation. Finally a series of simulations aimed to simulate the infra red heating system and the convective cooling system, necessary to control the heating process, achieving the ideal temperature distribution, more efficiency, energy saving and higher modularity with respect to the state of the art.

Keywords: Blow-molding machine, irradiating oven, PET, heat transfer, turbulent air flow.

1. Introduction

PET blow molding machines are the most popular technology employed to produce bottles and flagons. The process starts with the production of the PET, which is then used to make preforms that will be finally transformed into bottles. This paper will focus on the heating process of the preforms that leads to the final blow-molding transformation. The heating process is controlled through a series of panels, mounting Infra Red lamps, and the cooling airflow generated by dedicated fans. In fact one of the main issues in this transformation process is the temperature distribution along the preform length and the radial thickness, which should ideally vary according to the shape of the preform and the mechanical stresses introduced by the stretching action [1]. Consequently the main objective of this development was to design an oven which gave the possibility of a fine regulation of the temperature in the PET section with a particular attention for the critical regions. The deep level of knowledge reached with this simulation work will lead to the production of better quality bottles, thanks to a higher level of reliability of the process, whilst also savings on production waste. This study had been lead as a joint venture between SMILAB S.r.l. and SMIGROUP S.p.a., respectively a private research organization and a molding machines producer company and POLIBRIXIA S.r.l. an applied research consultancy studio.

2. Problem Definition

The heating process starts with the preforms running into a long oven chamber, the most diffused topology of industrial machines generally allocates on one side of the oven the batteries of IR lamps. In addition a ventilation system is used to control the heating process (Figure 1).

Figure 1. Photo of one IR lamp panel with preforms placed in front of it [SMI Group S.p.a.].

In order to enhance of the overall performances of the machine it is important to have a fine control of the variables that influence the production process. In fact, as previously introduced, the temperature distribution in the PET section depends on the axial and hoop stretching ratios [1], they are defined respectively as (Figure 2):

$$SR_A = \frac{L_B - 5}{L_P - 5} \quad (1)$$

$$SR_H = \frac{\emptyset_B}{\emptyset_P} \quad (2)$$

All the dimensions are expressed in *mm* and the lengths are reduced by *5mm* to consider the unvaried part of the bottleneck under the thread. The diameters can be measured as internal, external or a mean of the two, coherently with bottle and preform. It is also possible to define the blow-up stretching ratio as the multiplication between the two former ratios:

$$SR_{BU} = SR_A \times SR_H \quad (3)$$

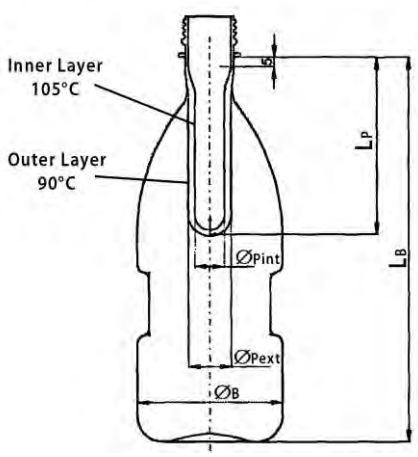

Figure 2. Stretching ratios and ideal internal and external preform surface temperature [1].

The most common blow-up stretching ratios used in the industrial production are comprised between 9.5 and 12, beyond this limit the stretching becomes difficult, with very tight temperature ranges and distributions [1]. For these ratios the useful temperature range is enclosed between 90 °C and 115 °C. Nevertheless with the industrial process it is difficult to reach the optimal temperature distribution, considered to have a decreasing gradient from 105 °C on the internal surface to 90 °C on the outer surface of the preform (Figure 2). This is due to a natural effect of the irradiation process, the temperature on the external surface results to be higher because of the superior IR energy absorption in the most outer PET layers.

Another issue to consider for the design is the uniformity of the longitudinal distribution. For non-uniform cylindrical bottles, the temperature should increase where the stretching is higher due to the bottle diameter variations. With the common industrial design it is hardly possible to decouple the effects of the adjacent IR lamps, consequently the system results in having a poor longitudinal temperature regulation.

The new design has therefore to include the possibility to modulate the longitudinal temperature distribution as well as the heat penetration in the PET section.

3. Model

The study of this problem is constituted of two main physical phenomenons, the preform heating induced by the irradiating panels and the cooling convection used to reduce the temperature on the external perform surface.

3.1 Assumptions

The model introduced in this section had been established under the following assumptions:

1. The air flow is turbulent around the performs inside the oven chamber due to the wide flow cross section and the air speed, resulting in a Reynolds number about 27,000. The turbulence is also increased by the presence of many boundary disturbances, such as obstacles on the walls, presence of preforms in translation and rotation along their longitudinal axis.

2. The preforms are rotating along their longitudinal axis while translating in front of the irradiating panels. Assuming that the dynamics of the thermal conduction within the PET section is slower than the thermal irradiation absorption, it's possible to consider the perform static exposed to a mean circular irradiating source. This is due to the high thermal conductive inertia of the PET and it is also in agreement with a simulation presented in the 4th section.

3.2 Data Gathering

Data collection started with the research of the PET physical properties in the literature. The second phase was the realization of the thermal absorption process simulation with the software Zemax and the importation of the results in COMSOL.

3.2.1 PET Properties

The production process of the preforms results in an amorphous structure of the PET, which is characterized by transparency, hardness, and fragility, at low temperature and high deformability at moderate temperature (about 100 °C). In this condition the material presents a Density of 1,370 g/cm^3, a Heat Capacity at constant pressure of 1000 J/(kg·K) [2] and a Thermal Conductivity of 0.15 W/(m·K) [3]. These values can vary depending on the characteristic of the material's production process; consequently this study had been conducted by using literature values that can be relevant as a qualitative reference for the industrial practice.

3.2.2 Geometrical Optics and IR Heating Design

The design of the optical IR system had been conducted using Zemax, this gave the possibility to model all the components of the system: the IR lamps USHIO QIH400-2500/ZH, the mirrors and the preforms. The simulations considered a battery of 6 lamps, coupled with mirrors, for a fine modular heating of the preforms and aimed to obtain an increment of the opto-thermal efficiency. The simulation studied the behavior of the IR rays produced by the lamps and how they were absorbed by the PET preform. The volume of the preform was divided into 125,000 voxels used as probes to evaluate the thermal power acting on the volume. To simplify the number of elements, the results of this 3D matrix had been imported calculating the mean power absorbed by the concentric ring slices during one turn in front of the lamps (section 4.1). In fact the new thermal source model had been realized dividing the cylindrical preform into slices and each slice into concentric rings. The results showed the absorption to be prevalent in the first external layers of material, with a behavior similar to the one visible in Figure 7 for the time 1.06s.

3.3 Governing Equations

The numerical problem studied with COMSOL concerned the two main aspects of the physics involved. The PET absorption of IR rays had been studied in Zemax and imported as a thermal power source in COMSOL. Consequently the following sections illustrate the main equations used for the analysis of thermal conduction within the PET section, the fluid dynamics of the cooling airflow and the related convection effect.

3.3.1 Heat Transfer

The main equation used to address this study is the first law of thermo dynamics [4]:

$$\rho C_P\left(\frac{\partial T}{\partial t}+(\boldsymbol{u}\cdot\nabla)T\right)=-(\nabla\cdot\boldsymbol{q})+\tau:\boldsymbol{S}-\frac{T}{\rho}\frac{\partial\rho}{\partial T}\Big|_p\left(\frac{\partial p}{\partial t}+(u\cdot\nabla)p\right)+Q \qquad (4)$$

Where ρ is the density, C_p is the heat capacity, T is the absolute temperature, $\boldsymbol{u}$ is the velocity vector, $\boldsymbol{q}$ is the heat flux by conduction, p is the pressure, τ is the viscous stress tensor, Q contains heat sources other than viscous stress and $\boldsymbol{S}$ is the strain-rate tensor calculated as:

$$\boldsymbol{S}=\frac{1}{2}(\nabla\boldsymbol{u}+(\nabla\boldsymbol{u})^T) \qquad (5)$$

This equation was used for the computation of the conductive thermal effect in the forced airflow and for the convective thermal exchanges with the PET heated preform. Therefore the velocity vector had been calculated with the numerical resolution of the turbulent fluid dynamic model.

Regarding the computation of the conduction that occurred in the PET section, the equation used was a simplified version of (4), where the velocity vectors, the stress factor of the fluid disappeared [4]:

$$\rho C_P\left(\frac{\partial T}{\partial t}\right)-\nabla(\mathrm{k}\cdot\nabla\mathrm{T})=Q \qquad (6)$$

Where k is the thermal conductivity and Q had been used as the thermal source to introduce the IR absorption into the model. All units of the variables are expressed according to the SI. The heat transfer component had been resolved as a

time dependent problem, since the objective is to simulate the process to optimize the new design.

3.3.2 Turbulent Air Flow

The assumption of turbulent model, seen in the section 3.1, had been taken into account referring to the common industrial practice. The reason this type of flow is adopted is that thanks to the presence of turbulence and vortexes, the forced convective effect resulted to be more efficient with respect to a laminar flow [5].
The object of this study was time invariant, to determine the velocity field to apply for the thermal exchange problem.
The main mathematical structure modeling this phenomenon is the Navier-Stokes equation for compressible flows (7), although this required high computational power to compute the solution for a wide range of flow scales. Consequently just the large scale flows were resolved, while the smaller ones were addressed using dedicated turbulence models [4].

$$\rho\left(\frac{\partial \boldsymbol{v}}{\partial t} + \boldsymbol{v}\cdot\nabla\boldsymbol{v}\right) = -\nabla p + \mu\nabla^2\boldsymbol{v} + \left(\frac{1}{3}\mu + \mu^v\right)\nabla(\nabla\cdot\boldsymbol{v}) + f \qquad (7)$$

In the previous equation, v is the flow velocity, ρ is the fluid density, p is the pressure, μ is dynamic viscosity, μ^v is the bulk viscosity and f represents external forces [6].
The numerical model used for the resolution was the standard k-ε model, which is often used for industrial applications since it is a fair trade off between the limited accuracy [7] and the amount of computational resource needed.
In this model two additional transport equations are introduced, the turbulent kinetic energy k and the dissipation rate of turbulence energy ε.

4. Study and Design

4.1 Study of the Thermal Source Model

The design started with a study of the thermal source generated inside the PET section thanks to the IR absorption. Since the number of voxels used to describe the phenomenon in Zemax was 125,000, it had been considered possible to divide the PET section in regions where a mean thermal source had been implemented. In order to achieve this modeling with a good approximation an analysis of the dynamic of absorption and conduction processes had to be performed. The assumption was that, while the preform is in front of the IR lamps, the energy is absorbed mostly in the front. However, when the preform is rotating around its longitudinal axis, it exposed a new section of its surface to the IR lamps. At this point if the spinning velocity (about 60rmp) resulted to be high enough, the total absorption per turn would have resulted similar to the mean absorption calculated on one turn.
To demonstrate this concept a simulation had been conducted using a 2D model of the section of the PET preform. The "ring" had been divided into 2 sections, with consideration to have air inside the empty space. At this point in the first simulation a rotating thermal source per ring, of area about 1mm^2, had been put in rotation on the PET section. The external heat source had been considered to be 9 mW, while the internal one 3 mW. In the second simulation the power of 9 and 3 mW had been dived by 75 and 69: the number of voxels present in the rings.
Simulating the heating process on one turn with a frequency of 1 Hz, showed that there was no relevant difference between the rotating case and the mean one (Figure 3).

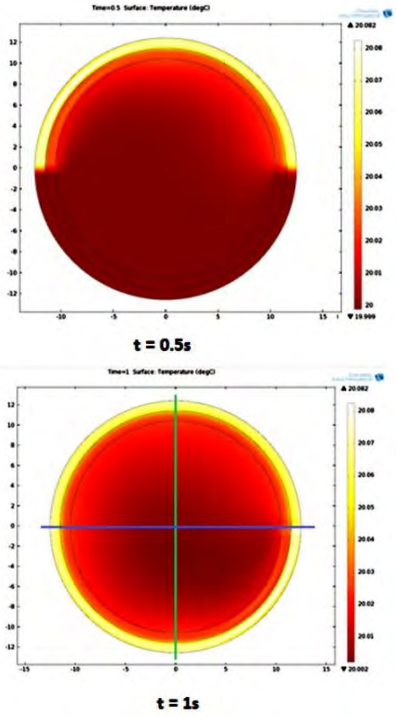

(a)

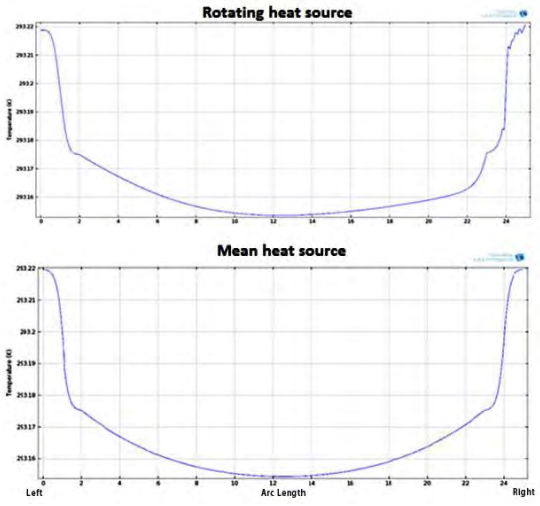

(b)

Figure 3. (a) Images representing the temperature distribution for the rotating source at 0.5s (left) and 1s (right). (b) Images representing the temperature distribution in the PET section for the rotating (above) and mean (below) heat sources, following the horizontal measuring line.

In fact as visible in the previous pictures, the temperature distribution follows the same path for both cases. There is just a slight difference on the right side of the image, which is the departure and arriving point of the rotating thermal source that consequently illustrates that the diffusion process had started again. The simulation had then extended to a longer period, simulating the real heating process of the preforms and showing the same behavior previously described.

The results gave the possibility to continue to develop the model with the assumption of a mean thermal absorption calculated on one turn of preform in front of the IR lamps, for each voxel. Finally this tridimensional matrix had been imported in COMSOL. This phase had been implemented in an iterative way, since it depended on the design of the optical system of the radiating panel.
The optical design needed to be validated by simulating the heating efficiency and the quality of the thermal distribution to obtain the best trade-off between performances and system complexity.

4.2 Study of the Fluid-Dynamics

Once the thermal absorption model had been defined, it was necessary to study the fluid-dynamic behavior of the ventilation inside the oven cavity. The adopted strategy consisted in taking the industrial state of the art as a reference model (in particular the SMI model SR8). This phase had been conducted to identify all the boundary effects that were relevant for the oven performances.

The first boundary effects considered were the translation and rotation of the preforms while exposed to the convective flow in the SR8. Considering the translation case, the linear velocity of the preforms in the oven was 0.16m/s, while in the case of the preforms rotation they turned at a frequency of 1Hz with a diameter of 21mm (and PET thickness of 2mm), generating a tangential speed of 0.066m/s. Since the convective flow mean speed (aspiration from the bottom of the cavity) was attended to be more than 20 times higher than the linear velocity, these components had been hypotized to be irrelevant for the modeling. The results of the simulations agreed with the assumptions, also showing that these boundary effects slightly increased the level of the turbulence in the oven cavity, increasing the convective efficiency. They are not reported here, as they are part of the assumptions for the final modeling.

Another boundary effect taken into account was the presence of fans dedicated to the cooling of the IR lamp heads. As in the previous case, the disturbance introduced resulted to be small and also localized at the extremities of the panels mounting the IR lamps. Furthermore the decision was not to model this part also because it had been planned to cool the heads of the lamps with the same convective flow, in order to eliminate the issue and reduce the number of fans employed in the system.

The final model to study the internal fluid dynamics of the oven panels considered the presence of an air injection from the top of the panel (Inlet), an aspiration from the bottom of the panel (Outlet) and a condition of symmetry at the entrance and exit of the panel.

Since the design followed an iterative procedure, several static simulations at different flow rates were developed to find the best solution for the thermal problem. The air flow had been generated by imposing a depression (about 300 Pa) at the bottom of the panel, simulating an aspirator fan, a light pressure (about 40Pa) had been applied also at the "Inlet" point to favorite a uniform distribution of the air flow around the preforms. The average rate of the aspiration airflow was 300m^3/h and the injection had been simulated with symmetric and asymmetric configurations (Figure 4).

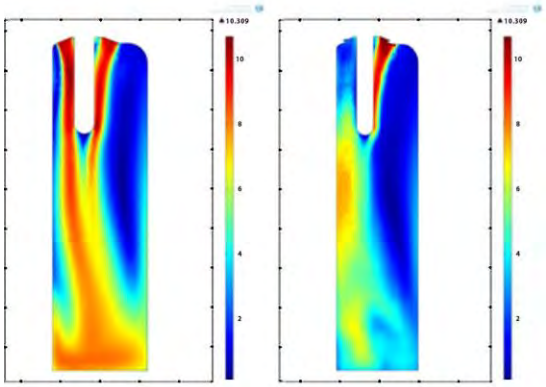

Figure 4. Lateral view of the results of the fluid dynamic simulation: symmetric strategy (left) and asymmetric strategy (right).

As visible in Figure 4, the color map represents the module of the air speed. The mean value obtained near the preform resulted to be about 10 m/s while mixing and slowing towards the final aspiration. The results also showed a high level of turbulence and vortexes in the upper part of the oven panel, due to a bigger volume for the recycling of the air. The IR lamps shown in Figure 1 are placed on the right side of the panel.

4.3 Combined study and final design

The results seen in the previous section had been used for the final study with the combination of thermal and fluid problems. This simulation represented the base of the new design, which consequently aimed to reproduce an industrial cycle of the heating process. In fact when the preform started their journey inside the oven chamber, it crossed some irradiating panels until it reached the curve, where there was no heating system. Once back on the linear track, the heating restarted until the preform temperature was ideal for the stretch-blowing (Figure 5).

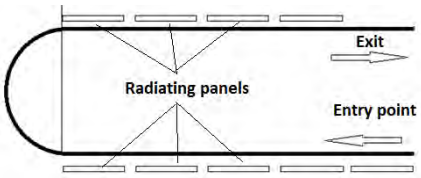

Figure 5. Scheme of the new industrial heating cycle.

The modular use of each panel gave the freedom to heat the preform following the best recipe accordingly to the type of bottle to produce. It was composed by a series of heating and cooling phases that lead the preform to reach a temperature distribution similar to the ideal one.

An interesting aspect of the thermal exchange occurred in the Cooling Phase 3, where radial temperature distribution had been inverted thanks to the convective flux (Figure 6).

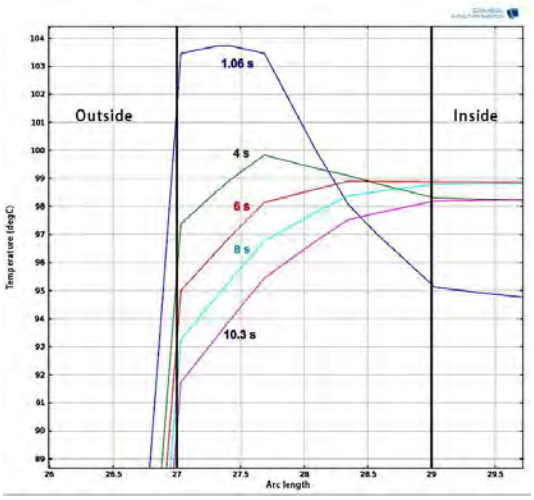

Figure 6. Radial temperature distribution measured at half of the preform length, during the Cooling Phase 3, at different times.

The curve representing the 1.06s temperature distribution represents clearly the way that PET absorbs external IR rays. The 1st millimeter of section absorbs almost 80% of the heat.
Another interesting thing is that thanks to the presence of air at lower temperature inside the

preform, a “heat-sink” phenomenon is generated and attracts the heat towards the centre. In fact the temperature on the internal surface results to be about 4 °C higher after the cooling phase, while the external one has dropped about 10 °C. As clear from the results the temperature distribution is already closed to the ideal one, which is possible to reach with the following heating and cooling phases (Figure 7).

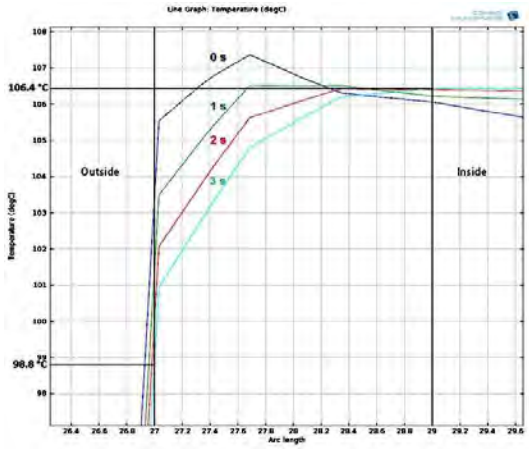

Figure 7. Radial temperature distribution measured at half of the preform length, during the Cooling Phase 4, at different times.

5. Results and Discussion

This section summarizes the improvements obtained with the new design. Starting from the energy consumption the efficiency of the thermal-optical component of the system had been increased from the 10.5% of state of the art (Model SR8 by SMI) to 24.1% with the new design. This had been achieved thanks to the mirror optical system that reduced the amount of energy lost in the oven environment. Another important advantage in terms of reduction of the energy consumption is the introduction of a thermal exchanger that gave the possibility of re-use the heat extracted from the oven panels to stabilize the temperature inside the machine and realize a climatic chamber insensitive to the external environmental and weather conditions.

Regarding the optical system there are several improvements obtained, with the new design it had been possible to achieve a better efficiency, as already mentioned, a customizable longitudinal and radial temperature distribution and a higher depth of thermal absorption in the PET section. The good modularity of the radiating panels favorited also a good uniformity in the temperature distribution and also it gave the possibility to cure with particular care critical parts (i.e. the bottleneck or bottom) of the preform. The new system reduced also the reciprocal influence of the heating lamps, this lead to a better management of the single lamp power as it became easier for the final user to obtain the desired result. Finally the new radiating panels have a geometrical configuration that let to keep the IR lamps more distant from the translation line of the preforms, this reduced the risk of lamp rupture due to the movement of the preforms.

Concerning the ventilation system, thanks to the simulations it had been possible to realize a system with more uniformity in the velocity field of the air flow, increasing the reliability of the quality level of the oven performances. This had been achieved by removing the boundary disturbances like the lateral ventilation, by introducing a correct ventilation and finally by developing a design that optimized the trade-off between space required and flux uniformity. Another improvement was that the main ventilation also cooled the head of the IR lamps, reducing the amount of components needed, like dedicated fans. Finally the new ventilation strategy, thanks to the thermal inversion, resulted to achieve the optimal thermal distribution in a shorter time and in a more deterministic way, with respect to the state of the art.

The benefits resulting from this study concerned as well the overall knowledge of the process, in fact it lead to study in detail the properties of each component of the system, from the PET preforms in terms of geometry and material properties, to the behavior of the optic and ventilation systems. Thanks to the better knowledge of the influence of the process variables, it has possible to define a control strategy for all the components of the system, since the modularity let to control the fans and lamps of each panel independently. The modularity increased also the efficiency and the handiness of the production and maintenance of the system, reducing the failure risk. Since the reliability and the stability of the new design had been significantly increased, it’s possible to develop for each type of preform common

recipes that will be the same wherever the machine will be employed, reducing the set up and tuning time for the beginning of a new production.
The study also involved the consultation of experts of the sector and the simulations results agreed with the industrial practice relatively to the state of the art simulations. The first prototype is now under construction and soon it will be tested.

6. Conclusions

With this study it had been possible to study in detail the thermal properties of the PET, in particular it had been demonstrated how for the industrial practice it is important to consider that the thermal conduction dynamic is much slower than the IR absorption. This underlined the need of having a robust cooling system which can favorite the heat penetration inside the PET section during the heating phases and the thermal inversion during the cooling phases. The fluid-dynamic simulation let to design a ventilation system with a high level of velocity field uniformity around the preforms, which lead to a simplified use of the variable flow speed. Furthermore with the combined simulations it had been possible to replicate a whole industrial cycle and estimate the feasibility in terms of resources and dimensions needed to implement the new design. Finally a prototype is being built by SMI Group, which incorporates all the advantages and features presented in the Section 5. With a good level of confidence it is possible to predict that the results of the prototype test will be close to the simulations, since for the "state of the art" it had been confirmed during the first phases of this study. In future it will be also possible to implement the model here presented as a base to study different recipes accordingly to the shape of the preform and bottle, reducing drastically the setting and tuning time for the beginning of the production of a new product.

7. References

1. O. Brandau, Stretch Blow Molding, Elsevier, ISB 978-1-43-773527-7, p.73-75, (2012).
2. A.K. van der Vegt & L.E. Govaert, Polymeren, van keten tot kunstof, ISBN 90-407-2388-5, (2005)
3. J. G. Speight, Norbert Adolph Lange (2005). McGraw-Hill. ed. Lange's handbook of chemistry (16 ed.). pp. 2.807–2.758. ISBN 0-07-143220-5, (2005).
4. COMSOL Heat Transfer Module User Guide, p. 171 (May 2011) and COMSOL CFD Module Users Guide, ps.156, (May 2011).
5. D. Pnueli, C. Gutfinger, Meccanica dei fluidi, ISBN 88-08-09388-3, p.322-324, (1995).
6. L. D. Landau, E. M. Lifshitz, Course of Theoretical Physics, Vol. 6 : Fluid Mechanics 2, nd, Ed., Pergamon Press, p.44-45 (1987)
7. D. M. Driver and H. L. Seegmiller, "Features of a Reattaching Turbulent Shear Layer in Diverging Channel Flow," AIAA Journal, vol. 23, pp. 163–171, (1985).

8. Acknowledgements

This work wouldn't have been realized without the precious technical sustain of Marco Grazioli and Giorgio Salvi and Paolo Nava of SMIGroup. A special thanks is for Paolo Tommasini, of Q-Tech, for the design and simulation of the optical component of the oven and a special thank also to Dott. Canali for the theoretical basis on PET blow molding.